

## COMMUNICATION

[View Article Online](#)  
[View Journal](#) | [View Issue](#)Cite this: *Dalton Trans.*, 2024, **53**, 15795Received 20th August 2024,  
Accepted 12th September 2024

DOI: 10.1039/d4dt02372b

[rsc.li/dalton](https://rsc.li/dalton)Analogous carbene-stabilised  $[M^I-(\eta^6\text{-tol})]^+$  cations ( $M = \text{Fe, Co, Ni}$ ): synthetic access and  $[\text{carbene}\cdot M^I]^+$  transfer†

Annika Schulz and Terrance J. Hadlington \*

A series of low-coordinate cationic 3d metal(I) complexes of the general formula  $[\text{IPr}\cdot M(\eta^6\text{-tol})]^+$  is reported ( $M = \text{Fe, Co, Ni}$ ;  $\text{IPr} = [(\text{H})\text{CN}(\text{Dip})\text{C}]$ ;  $\text{Dip} = 2,6\text{-}^i\text{Pr}_2\text{-C}_6\text{H}_3$ ), employing the weakly coordinating  $[\text{BAR}^F_4]^-$  counter-anion. The central metal in these complexes is stabilised solely by neutral carbene (*i.e.* IPr) and arene (*i.e.* toluene) ligands, making them rare examples of such cationic 3d metal(I) complexes, the electronic nature of which is explored by SQUID magnetometry. The utility of these species in  $[\text{IPr}\cdot M^I]^+$  transfer chemistry is demonstrated through the addition of a further equivalent of IPr, leading to formally two-coordinate cationic complexes,  $[(\text{IPr})_2\cdot M^I]^+$ .

Low-valent, low-coordinate 3d transition metal (TM) complexes have garnered significant interest owing to their typically high reactivity,<sup>1–4</sup> and more recently their potential as single-molecule magnets.<sup>5,6</sup> Whilst historically cyclopentadienyl and carbonyl ligands have dominated the space of organometallic TM chemistry,<sup>7–10</sup> their high electron donor number and small size, respectively, do not favour low coordination numbers. Here, N-heterocyclic carbenes (NHCs) have played a key role,<sup>1,11–13</sup> allowing for the synthesis of stable electron deficient TM complexes through strong  $\sigma$ -donation and bulky, tunable steric properties. This has shone particularly true for Ni,<sup>14</sup> as pioneered by Hartwig and co-workers, whereby a large NHC ligand drives catalytic turn-over in, for example, hydrogenative aryether scission,<sup>15,16</sup> and alkene hydroarylation using well-defined  $\text{Ni}^0$  pre-catalysts.<sup>17</sup> Significant efforts have thus gone towards for the synthesis of reactive low-valent NHC-stabilised 3d metal complexes. Key examples are the dvtms-bound  $M^0$  complexes  $[\text{NHC}\cdot M(\text{dvtms})]$  (Fig. 1(a);  $\text{NHC} = \text{IPr}$ ,  $M = \text{Fe, Ni}$ ;  $\text{IPr} = [(\text{H})\text{CN}(\text{Dip})\text{C}]$ ;  $\text{Dip} = 2,6\text{-}^i\text{Pr}_2\text{-C}_6\text{H}_3$ ;  $\text{NHC} = \text{IMes}$ ,  $M = \text{Co}$ ;  $\text{IMes} = [(\text{H})\text{CN}(\text{Mes})\text{C}]$ ;  $\text{Mes} = 2,4,6\text{-Me}_3\text{-C}_6\text{H}_2$ ;

$\text{dvtms} = 1,3\text{-divinyltetramethyldisiloxane}$ ),<sup>18–20</sup> which are both effective catalysts as well as  $[\text{NHC}\cdot M^0]$  transfer reagents.<sup>3,21</sup> This latter point has been thoroughly explored by Deng and co-workers, for example in the exploration of low-coordinate Fe and Co imido species.<sup>22–24</sup> Indeed, the same group later reported the related  $\text{Mn}^0$  complex,<sup>25</sup> in addition to vtms-coordinated examples for Fe and Co (vtms = vinyltrimethylsilane),<sup>22,24</sup> which show improved reactivity due to the ease of loss of vtms. Beyond alkene-stabilised systems, arene complexes have also seen some attention (*e.g.* Fig. 1(b) and (c)), which have potential benefits due to the chemical innocence of an arene leaving group. In this regard, Hillhouse, Cundari and co-workers demonstrated the straightforward access to a nickel-imide featuring a two-coordinate Ni centre.<sup>26</sup> More recently, Deng and co-workers reported the cationic  $\text{Co}^I$  complex  $[\text{IPr}\cdot \text{Co}(\eta^6\text{-C}_6\text{H}_5)\text{BPh}_3]$ , in which the coordinated

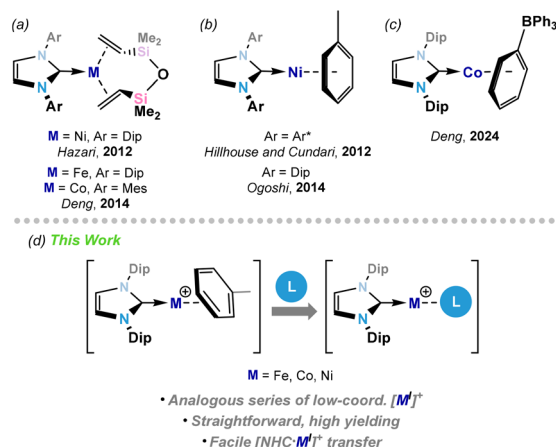


**Fig. 1** Key reported examples of (a) (dvtms)-complexes of NHC- $M^0$  moieties, (b) simple arene complexes of NHC- $\text{Ni}^0$  moieties, and (c) a cationic arene complex of  $\text{Co}^I$ ; (d) this work, demonstrating the facile access to arene adducts of cationic  $[\text{NHC}\cdot M^I]^+$  moieties, and their utility in  $[\text{NHC}\cdot M^I]^+$  group transfer.

Lehrstuhl für anorganische Chemie mit Schwerpunkt neue Materialien, School of Natural Sciences, Technische Universität München, Lichtenberg Strasse 4, 85747 Garching. E-mail: [terrance.hadlington@tum.de](mailto:terrance.hadlington@tum.de)

† Electronic supplementary information (ESI) available. CCDC 2377592–2377597. For ESI and crystallographic data in CIF or other electronic format see DOI: <https://doi.org/10.1039/d4dt02372b>

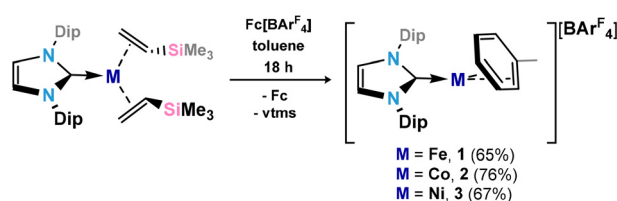
$[\text{BPh}_4]^-$  ion can be displaced by various different neutral ligands.<sup>27</sup>

In our work, we have utilized the  $\text{M}^0$  species  $[\text{IPr-M}(\text{vtms})_2]$  as  $[\text{IPr-M}^0]$  transfer reagents in forming a range of heavier triylene- and tetrylene-ligated 3d metal complexes ( $\text{M} = \text{Fe}, \text{Co}, \text{Ni}$ ).<sup>28–31</sup> We sought to develop an analogous family of cationic  $\text{M}^1$  systems, *viz.*  $[\text{IPr-M}]^+$ , which may be useful to the organometallic chemistry community as ubiquitous  $[\text{NHC-M}]^+$  transfer reagents. Herein we describe our efforts in this direction. Specifically, we report the synthesis of  $\text{Fe}^1$ ,  $\text{Co}^1$ , and  $\text{Ni}^1$  cations, stabilised by the bulky carbene IPr, and toluene. The electronic nature of these species is elucidated using SQUID magnetometry, and their utility as synthons of the  $[\text{IPr-M}]^+$  fragment is demonstrated through their reaction with a further equivalent of carbene.

## Results and discussion

In seeking reactive  $[\text{IPr-M}]^+$  transfer reagents, we sought the one-electron oxidation of known  $[\text{IPr-M}^0]$  reagents. To this end, the oxidation of  $[\text{IPr-M}(\eta^2\text{-vtms})_2]$  systems ( $\text{M} = \text{Fe}, \text{Co}, \text{Ni}$ ) with  $\text{Fc}[\text{BAR}^{\text{F}}_4]$  ( $\text{Fc} = \text{ferrocene}$ ;  $\text{Ar}^{\text{F}} = 3,5\text{-CF}_3\text{C}_6\text{H}_3$ )<sup>32</sup> in toluene rapidly led to the deposition of deep purple (Fe), green (Co), or yellow (Ni) oily solids (see ESI† for details), beneath an orange

solution (Scheme 1).  $^1\text{H}$  NMR spectroscopic analysis of the supernatant reaction solutions in all cases indicated the formation of free Fc and vtms, and disappearance of signals relating to the IPr ligand. Single crystals of compounds **1** (Fe), **2** (Co), and **3** (Ni) could be grown from the described coloured oils by layering of their fluorobenzene solutions with pentane, revealing that in all cases toluene complexes,  $[\text{IPr-M}(\eta^6\text{-tol})][\text{BAR}^{\text{F}}_4]$ , are formed. All species crystallise in the  $P2_1/n$  space group, and are essentially isostructural (Fig. 2). The  $\text{C}^{\text{NHC}}\text{-TM}$  distance contracts on moving from Fe to Ni ( $d_{\text{C1Fe1}} = 2.034(3)$  Å;  $d_{\text{C1Co1}} = 1.994(3)$  Å;  $d_{\text{C1Ni1}} = 1.929(3)$  Å), whilst the opposite trend is observed for the average  $\text{C}^{\text{Tol}}$  distance (Fe: 2.149 Å; Co: 2.151 Å; Ni: 2.196 Å). Notably, and again in all cases, a ring-tilt of the toluene ligand is observed, relative to the  $[\text{IPr-M}]$  plane. This is primarily indicated by the non-linear  $\text{NHC-M-Tol}^{\text{centroid}}$  angle, which is most extreme for Co and Ni (Fig. 2 inset). This is further borne out by generally shorter  $\text{M-C33}$  (Fe: 2.142 Å; Co: 2.128 Å; Ni: 2.161 Å) and  $\text{-C34}$  (Fe: 2.139 Å; Co: 2.118 Å; Ni: 2.211 Å) contacts when compared with related  $\text{C30}$  (Fe: 2.148 Å; Co: 2.182 Å; Ni: 2.212 Å) and  $\text{C31}$  (Fe: 2.153 Å; Co: 2.175 Å; Ni: 2.311 Å) contacts. Now, when taking the centroids  $[\text{C34-C29}]$  and  $[\text{C33-C32}]$  as binding points for the  $\text{M}\cdots\text{Tol}$  interaction, one finds what can be considered a *pseudo-Y-shaped* geometry at Fe, Co, and Ni, again most prominently for the latter two metals. That is, angles at M pertain to planarity ( $\sum\angle_{\text{M}} = 355.97^\circ$ ;  $\sum\angle_{\text{Co}} = 359.69^\circ$ ;  $\sum\angle_{\text{Ni}} = 359.95^\circ$ ),  $\text{C1-M-centroid}$  angles lie between  $142^\circ$  and  $157^\circ$ , and centroid-M-centroid angle are between  $60^\circ$  and  $62^\circ$ . A similar effect was noted in  $[\text{IPr-Co}(\eta^6\text{-PhBPh}_3)]$  reported by Deng *et al.*,<sup>27</sup> as well as in  $\text{IPr-CoCp}$ .<sup>33</sup> In the latter case, this phenomenon was presumed to be a result of steric hindrance; given that this tilting effect increases across the series Fe–Ni for analogous complexes, however, this is clearly an electronic effect. As such, and particularly for Co and Ni complexes **2** and **3**, we propose a formal  $\eta^4\text{-tol}$  binding mode in these species. All systems show clear  $\pi$ -stacking between their toluene ligand



**Scheme 1** Synthesis of cationic toluene complexes of Fe (**1**), Co (**2**), and Ni (**3**). Dip = 2,6- $i\text{-Pr}_2\text{-C}_6\text{H}_3$ ;  $\text{Ar}^{\text{F}} = 3,5\text{-(CF}_3)_2\text{-C}_6\text{H}_3$ ; Fc = ferrocene.

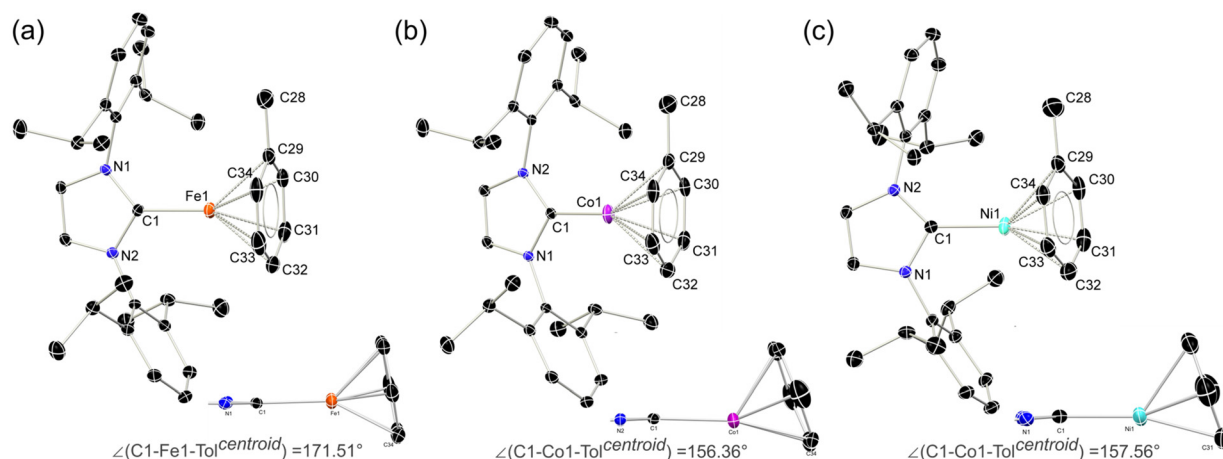


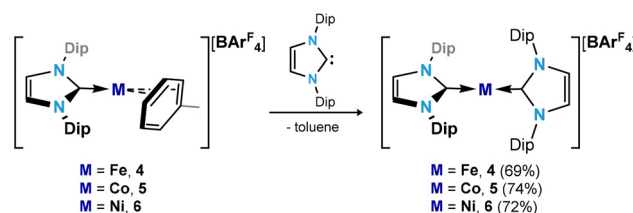
**Fig. 2** Molecular structure of the cationic part in (a) **1**, (b) **2**, and (c) **3**, with thermal ellipsoids at 30% probability, and hydrogen atoms removed for clarity. Inset: side-on view of the  $\text{NHC-M-tol}$  binding, demonstrating an increased tilt-angle in the  $\text{C1-M-Tol}^{\text{centroid}}$  centroid on moving from  $\text{M} = \text{Fe}$  to  $\text{M} = \text{Ni}$ .



and one  $[\text{Ar}^{\text{F}}]$  group of the  $[\text{BAr}^{\text{F}}_4]^-$  counter-ion, with  $\text{ToI}^{\text{centroid}}-\text{Ar}^{\text{F}}\text{C}^{\text{para}}$  distances of 3.560 Å (Fe), 3.589 Å (Co), and 3.582 Å (Ni). In all cases, no significant increase in C–C bond lengths are observed in the toluene ligands relative to a ‘free’ arene (average C–C bond length in **1**: 1.40 Å; in **2**: 1.39 Å; in **3**: 1.39 Å), which would suggest weak binding of these ligands.

All complexes exhibit highly broadened signals in their  $^1\text{H}$  NMR spectra, over a wide shift range (see ESI†), so demonstrating paramagnetic character. This is expected for **1** and **3**, which are  $d_7$  and  $d_9$  respectively. In addition, closely related  $[\text{IPr}\cdot\text{Co}(\eta^6\text{-PhBPh}_3)]$ , recently reported by Deng *et al.*,<sup>27</sup> is open-shell (*i.e.* high-spin) and paramagnetic, despite being  $d_8$  as per **2**. The described solid-state structures give potential information regarding the electronic nature of **1–3**, whereby Y-shaped geometries lead to five non-degenerate d-orbitals.<sup>34</sup> SQUID magnetometry yields room temperature  $\mu_{\text{eff}}$  values of 4.19, 3.98, and  $2.16\mu_{\text{B}}$  for **1**, **2**, and **3**, respectively. For **1**, this a clear indication of a high-spin  $\text{Fe}^{\text{I}}$  system, with  $S = 3/2$ , the observed value being only slightly higher than the spin-only value of  $3.88\mu_{\text{B}}$ . Equally, **3** demonstrates a near ideal  $\mu_{\text{eff}}$  for an  $S = 1/2$  system, fitting the proposed  $d^9$  electronic configuration. Complex **2**, on the other hand, has a significantly higher  $\mu_{\text{eff}}$  than expected for an  $S = 1$ , high-spin  $\text{Co}^{\text{I}}$  system, with a theoretical spin-only value of  $2.83\mu_{\text{B}}$ . This effect most likely arises from a significant spin–orbit coupling in this species and an incomplete coupling of orbital angular momentum.<sup>35</sup> Interestingly, the Evans method-derived  $\mu_{\text{eff}}$  for the same system as a solution in  $\text{D}_8\text{-THF}$  falls to  $2.85\mu_{\text{B}}$ , very close to the theoretical spin-only value, which may suggest some quench-

ing of spin–orbit coupling in solution. Of course, we cannot discount that THF coordination may play a role in a geometry change for this species in solution. Looking deeper into the magnetisation of these species, the magnetic susceptibility ( $\chi_{\text{M}}$ ) of **1** and **3** follows clear Curie–Weiss paramagnetic behavior (Fig. 3(d) and (f)), whilst that for **2** is indicative of antiferromagnetic coupling ( $\theta_{\text{CW}} = -24.2$  K; Fig. 3(e)). For all systems, a linear increase in magnetization with increasing field strength is observed at 300 K (Fig. S7, S15 and S23 in ESI†). Density Functional Theory (DFT) optimised structures for simplified modifications of **1–3**, *i.e.*  $[\text{IXyl}\cdot\text{M}(\eta^6\text{-benz})]$  (**1'**,  $\text{M} = \text{Fe}$ ; **2'**,  $\text{M} = \text{Co}$ ; **3'**,  $\text{M} = \text{Ni}$ ;  $\text{IXyl} = [(\text{H})\text{CN}(\text{Xyl})\text{C}]$ ;  $\text{Xyl} = 1,6\text{-Me}_2\text{-C}_6\text{H}_3$ ; Fig. S32–S34 in ESI†), yields structures in keeping with the general form observed in the X-ray crystal structures, for  $S = 3/2$ ,  $S = 1$ , and  $S = 1/2$  spin states for Fe, Co, and Ni, respectively. That is, a tilted and ‘slipped’ arene–M binding mode is observed, yielding what may be described as Y-shaped coordi-



**Scheme 2** Synthesis of cationic bis(NHC) complexes of Fe (**4**), Co (**5**), and Ni (**6**). Dip = 2,6- $^i\text{Pr}_2\text{-C}_6\text{H}_3$ ;  $\text{Ar}^{\text{F}} = 3,5\text{-(CF}_3)_2\text{-C}_6\text{H}_3$ .

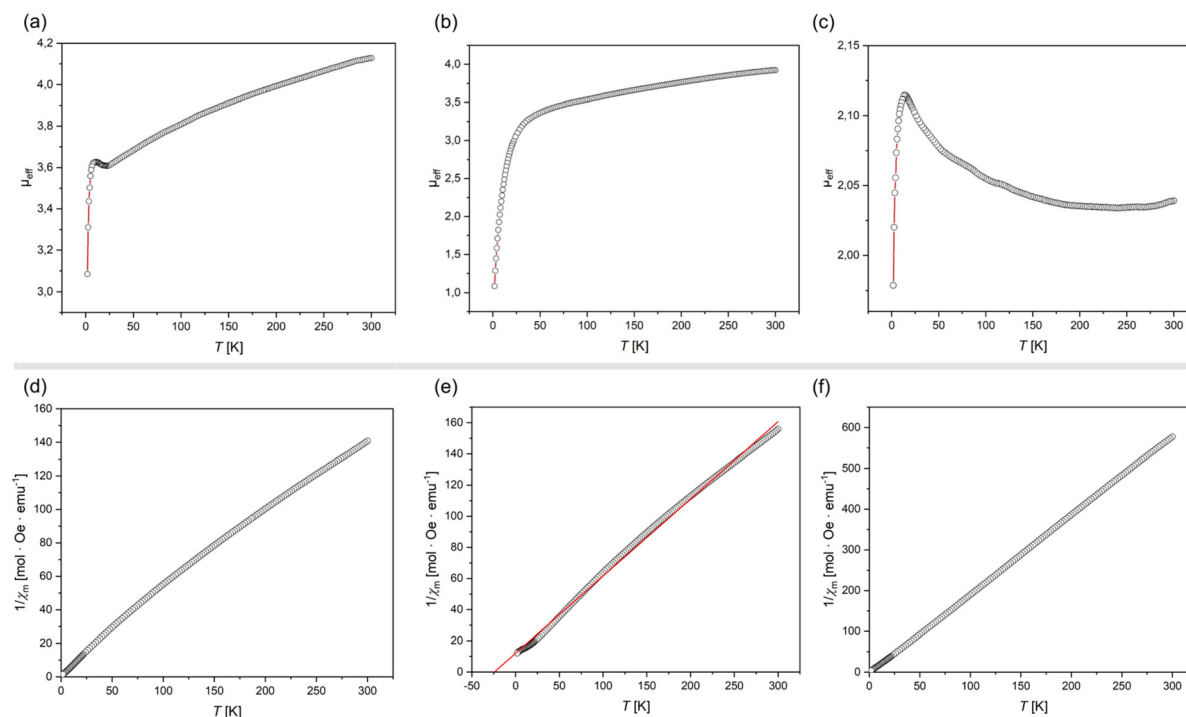


**Fig. 3** Plots of (a)–(c)  $\mu_{\text{eff}}$  vs.  $T$ , and (d)–(f)  $1/\chi_{\text{M}}$  vs.  $T$ , for complexes **1–3**.



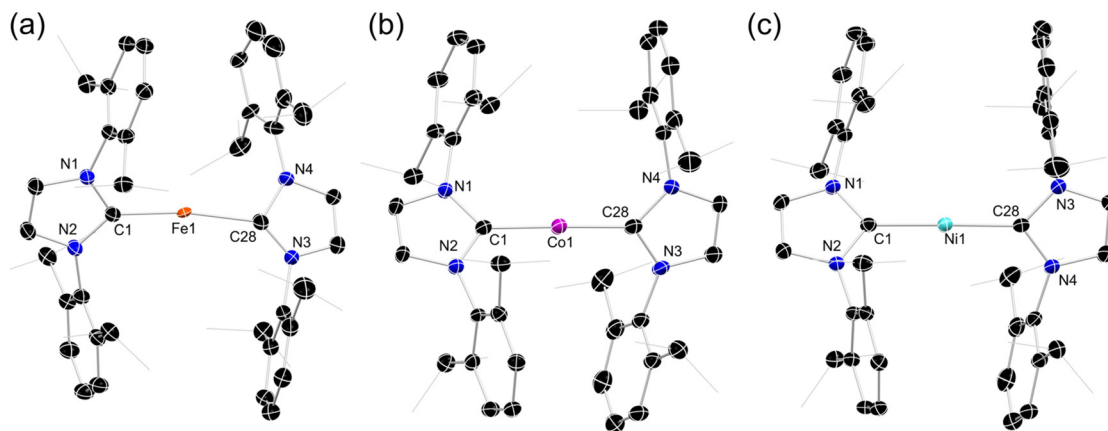


Fig. 4 Molecular structure of the cationic part in (a) **4**, (b) **5**, and (c) **6**, with thermal ellipsoids at 30% probability, and hydrogen atoms removed for clarity.

nation at M. Mulliken spin densities are localised at the M-centres in all cases (Fe: 3.00; Co: 2.00; Ni: 0.96), suggesting minimal delocalisation to the NHC or arene ligands.

Following the isolation of compounds **1–3**, we aimed to investigate their utility as  $[\text{IPr-M}]^+$  transfer reagents. To this end, a further equivalent of IPr was added to those species, targeting two-coordinate  $\text{M}^{\text{I}}$  cations, examples of which have seen interest in the literature as single-molecule magnets.<sup>36,37</sup>

Addition of IPr to  $\text{Et}_2\text{O}$  solutions of **1–3** led to dramatic colour changes in the formation of  $[(\text{IPr})_2\text{M}][\text{BAR}^{\text{F}}_4]$  complexes ( $\text{M} = \text{Fe}$  (**4**),  $\text{Co}$  (**5**), and  $\text{Ni}$  (**6**)), which can be isolated as deep red, orange, and colourless crystalline solids, respectively, in good yields of between 69 and 74% (Scheme 2). All could be crystallographically characterised, with their molecular structures shown in Fig. 4. As for toluene complexes **1–3**, complexes **4–6** are isostructural, crystallising in the  $P2_1/n$  space group and equal cell parameters. Still, slight differences are observed in their molecular structures: **5** and **6** feature essentially linear  $\text{C}^{\text{NHC}}\text{--M--C}^{\text{NHC}}$  angles of  $178.4(2)$  and  $178.8(2)^\circ$ , respectively, and are similar to their reported counterparts.<sup>36,38–40</sup> In contrast, this central  $\text{C}^{\text{NHC}}\text{--M--C}^{\text{NHC}}$  angle bends to  $170.4(2)^\circ$  in the iron(i) complex **4**. The  $\text{C}^{\text{NHC}}\text{--M}$  distances in this complex (*i.e.*  $2.035(4)$  and  $2.027(4)$  Å) are also longer than those found in **5** (*i.e.*  $1.990(5)$  and  $1.971(6)$  Å) and **6** (*i.e.*  $1.945(4)$  and  $1.934(5)$  Å), though this follows a similar trend as observed for **1–3**. All species are paramagnetic, borne out by the broad and wide-spanning  $^1\text{H}$  NMR spectra. A number of earlier reported two-coordinate cationic  $[(\text{NHC})_2\text{Fe}]^+$  systems,<sup>37,41</sup> two-coordinate anionic  $\text{Fe}^{\text{I}}$  species  $[(\text{Me}_3\text{Si})_2\text{HC}_2\text{Fe}]^-$  and  $[(\text{Me}_3\text{Si})_2\text{N}_2\text{Fe}]^-$ ,<sup>42,43</sup> and indeed Y-shaped toluene complex **1** demonstrate large solution-state magnetic moments, typically attributed to high-spin (*i.e.*  $S = 3/2$ )  $\text{Fe}^{\text{I}}$  with significant spin-orbit coupling and large magnetic contributions from unquenched orbital angular momentum. In contrast, the corresponding value for **4** is  $2.27\mu_{\text{B}}$ . This is now closer to that expected for an  $S = 1/2$  system, and would therefore suggest a low-spin  $\text{Fe}^{\text{I}}$  complex, apparently brought about by a simple

increase in steric bulk of the NHC ligand. This suggests that further exploration of bis(NHC) iron(i) species, analogous to **4**, may allow for tuning of electronic and magnetic properties. For this, toluene complex **1** seems an ideal candidate.

## Conclusions

In conclusion, we have described the synthesis, structure, and electronic nature of a series of  $\text{M}^{\text{I}}$  cations ( $\text{M} = \text{Fe}, \text{Co}, \text{Ni}$ ), stabilised by an NHC and a labile toluene ligand. All systems demonstrate a high-spin, open shell ground state. All systems also feature a tilted arene binding mode, becoming more prominent on moving from Fe to Ni, and pertaining to a form  $\eta^4$ -toluene binding mode for Co and Ni. These complexes have been utilized in the high-yielding  $[\text{NHC-M}]^+$  transfer reaction on combination with a further equivalent of carbene, leading to two-coordinate bis(NHC)  $\text{Fe}^{\text{I}}$ ,  $\text{Co}^{\text{I}}$ , and  $\text{Ni}^{\text{I}}$  cations. This study thus introduces a new readily accessible and analogous family of 3d-metal-cation transfer reagents, which we are exploring in their complexation behavior towards heavier low-valent *p*-block ligands.

## Author contributions

A. S. carried all experimental work. T. J. H. carried out computational evaluations, and conceived and supervised the project. A. S. and T. J. H. co-wrote the manuscript.

## Data availability

The ESI contains: Synthetic and analytical data for all new compounds; images of spectra for all new compounds; X-ray crystallographic information for structurally characterised species; computational details. In addition the





Crystallographic Information Files (CIFs) for 1–6 are freely available from the CCDC (numbers 2377592–2377597†).

## Conflicts of interest

There are no conflicts to declare.

## Acknowledgements

TJH thanks the Fonds der Chemischen Industrie (FCI) for generous funding of this research through a Liebig Stipendium, the ERC for a Starting grant (Project 101076897 – SINGAMBI), the DFG for an Independent Research grant (ProjectNr. HA9030/3-147032324, the Technical University Munich for the generous endowment of TUM Junior Fellow funds, and Prof. Fässler for his continued support. We also thank P. Mollik and J. Gilch for their help in acquiring LIFDI-MS data, and L. Kreimer for help in acquiring UV/vis data.

## References

- 1 L. J. Taylor and D. L. Kays, *Dalton Trans.*, 2019, **48**, 12365–12381.
- 2 P. P. Power, *Chem. Rev.*, 2012, **112**, 3482–3507.
- 3 Y. Liu, J. Cheng and L. Deng, *Acc. Chem. Res.*, 2020, **53**, 244–254.
- 4 A. Noor, *Coord. Chem. Rev.*, 2023, **476**, 214941.
- 5 J. M. Frost, K. L. M. Harriman and M. Murugesu, *Chem. Sci.*, 2016, **7**, 2470–2491.
- 6 A. Zabala-Lekuona, J. M. Seco and E. Colacio, *Coord. Chem. Rev.*, 2021, **441**, 213984.
- 7 M. Green and I. R. Butler, in *Organometallic Chemistry*, ed. M. Green, The Royal Society of Chemistry, 1st edn, 2004, pp. 393–444.
- 8 S. Lauk and A. Schäfer, *Eur. J. Inorg. Chem.*, 2021, **2021**, 5026–5036.
- 9 P. J. Dyson and J. S. McIndoe, *Transition Metal Carbonyl Cluster Chemistry*, CRC Press, 2018.
- 10 H. Nakazawa, in *Organometallic Chemistry*, ed. H. Nakazawa and J. Koe, The Royal Society of Chemistry, 2021, pp. 43–57.
- 11 F. Glorius, *N-Heterocyclic Carbenes in Transition Metal Catalysis*, Springer Berlin Heidelberg, Berlin, Heidelberg, 2007, vol. 21.
- 12 H. V. Huynh, *The Organometallic Chemistry of N-heterocyclic Carbenes*, Wiley, 1st edn, 2017.
- 13 G. G. Zámbo, J. F. Schlagintweit, R. M. Reich and F. E. Kühn, *Catal. Sci. Technol.*, 2022, **12**, 4940–4961.
- 14 V. Ritleng, M. Henrion and M. J. Chetcuti, *ACS Catal.*, 2016, **6**, 890–906.
- 15 A. G. Sergeev and J. F. Hartwig, *Science*, 2011, **332**, 439–443.
- 16 N. I. Saper and J. F. Hartwig, *J. Am. Chem. Soc.*, 2017, **139**, 17667–17676.
- 17 N. I. Saper, A. Ohgi, D. W. Small, K. Semba, Y. Nakao and J. F. Hartwig, *Nat. Chem.*, 2020, **12**, 276–283.
- 18 J. Wu, J. W. Faller, N. Hazari and T. J. Schmeier, *Organometallics*, 2012, **31**, 806–809.
- 19 L. Zhang, Y. Liu and L. Deng, *J. Am. Chem. Soc.*, 2014, **136**, 15525–15528.
- 20 H. Zhang, Z. Ouyang, Y. Liu, Q. Zhang, L. Wang and L. Deng, *Angew. Chem., Int. Ed.*, 2014, **53**, 8432–8436.
- 21 J. Dong, X. Leng, D. Wang and L. Deng, *ACS Catal.*, 2024, **14**, 4001–4007.
- 22 J. Du, L. Wang, M. Xie and L. Deng, *Angew. Chem., Int. Ed.*, 2015, **54**, 12640–12644.
- 23 X.-N. Yao, J.-Z. Du, Y.-Q. Zhang, X.-B. Leng, M.-W. Yang, S.-D. Jiang, Z.-X. Wang, Z.-W. Ouyang, L. Deng, B.-W. Wang and S. Gao, *J. Am. Chem. Soc.*, 2017, **139**, 373–380.
- 24 J. Cheng, J. Liu, X. Leng, T. Lohmiller, A. Schnegg, E. Bill, S. Ye and L. Deng, *Inorg. Chem.*, 2019, **58**, 7634–7644.
- 25 J. Cheng, Q. Chen, X. Leng, Z. Ouyang, Z. Wang, S. Ye and L. Deng, *Chem*, 2018, **4**, 2844–2860.
- 26 C. A. Laskowski, A. J. M. Miller, G. L. Hillhouse and T. R. Cundari, *J. Am. Chem. Soc.*, 2011, **133**, 771–773.
- 27 Q. Wang, X. Leng, D. Wang, S.-D. Bai and L. Deng, *Organometallics*, 2024, **43**, 689–694.
- 28 P. M. Keil, A. Soyemi, K. Weisser, T. Szilvási, C. Limberg and T. J. Hadlington, *Angew. Chem., Int. Ed.*, 2023, **62**, e202218141.
- 29 A. Schulz, T. L. Kalkuhl, P. M. Keil and T. J. Hadlington, *Angew. Chem., Int. Ed.*, 2023, **62**, e202305996.
- 30 P. M. Keil, S. Ezendu, A. Schulz, M. Kubisz, T. Szilvási and T. J. Hadlington, *J. Am. Chem. Soc.*, 2024, **146**, 23606–23615.
- 31 T. Kalkuhl, I. Fernández and T. Hadlington, *ChemRxiv*, 2024, DOI: [10.26434/chemrxiv-2024-hp230](https://doi.org/10.26434/chemrxiv-2024-hp230).
- 32 A. R. O'Connor, C. Nataro, J. A. Golen and A. L. Rheingold, *J. Organomet. Chem.*, 2004, **689**, 2411–2414.
- 33 J. M. Andjaba, J. W. Tye, P. Yu, I. Pappas and C. A. Bradley, *Chem. Commun.*, 2016, **52**, 2469–2472.
- 34 W. J. M. Blackaby, S. Sabater, R. C. Poulten, M. J. Page, A. Folli, V. Krewald, M. F. Mahon, D. M. Murphy, E. Richards and M. K. Whittlesey, *Dalton Trans.*, 2018, **47**, 769–782.
- 35 S. Mugiraneza and A. M. Hallas, *Commun. Phys.*, 2022, **5**, 95.
- 36 Y.-S. Meng, Z. Mo, B.-W. Wang, Y.-Q. Zhang, L. Deng and S. Gao, *Chem. Sci.*, 2015, **6**, 7156–7162.
- 37 Y.-S. Meng, Z. Ouyang, M.-W. Yang, Y.-Q. Zhang, L. Deng, B.-W. Wang and S. Gao, *Inorg. Chem. Front.*, 2019, **6**, 1050–1057.
- 38 S. C. Meier, A. Holz, J. Kulenkampff, A. Schmidt, D. Kratzert, D. Himmel, D. Schmitz, E. Scheidt, W. Scherer, C. Bülow, M. Timm, R. Lindblad, S. T. Akin, V. Zamudio-Bayer, B. von Issendorff, M. A. Duncan, J. T. Lau and I. Krossing, *Angew. Chem., Int. Ed.*, 2018, **57**, 9310–9314.
- 39 M. W. Kuntze-Fechner, H. Verplancke, L. Tendra, M. Diefenbach, I. Krummenacher, H. Braunschweig,



- T. B. Marder, M. C. Holthausen and U. Radius, *Chem. Sci.*, 2020, **11**, 11009–11023.
- 40 Z. Mo, D. Chen, X. Leng and L. Deng, *Organometallics*, 2012, **31**, 7040–7043.
- 41 Z. Ouyang, J. Du, L. Wang, J. L. Kneebone, M. L. Neidig and L. Deng, *Inorg. Chem.*, 2015, **54**, 8808–8816.
- 42 C. G. Werncke, P. C. Bunting, C. Duhayon, J. R. Long, S. Bontemps and S. Sabo-Etienne, *Angew. Chem., Int. Ed.*, 2015, **54**, 245–248.
- 43 J. M. Zadrozny, D. J. Xiao, M. Atanasov, G. J. Long, F. Grandjean, F. Neese and J. R. Long, *Nat. Chem.*, 2013, **5**, 577–581.

